Sensors and Actuators B 229 (2016) 646–654

Contents lists available at ScienceDirect

Sensors and Actuators B: Chemical

journal homepage: www.elsevier.com/locate/snb

Regenerative biosensor chips based on switchable mutants of avidin—A systematic study

Dominik Zauner[a], Barbara Taskinen[b,c], Daniel Eichinger[a], Clemens Flattinger[a], Bianca Ruttmann[a], Claudia Knoglinger[a], Lukas Traxler[a], Andreas Ebner[a], Hermann J. Gruber[a,*], Vesa P. Hytönen[b,c]

[a] Institute of Biophysics, Johannes Kepler University, Gruberstrasse 40, 4020 Linz, Austria
[b] BioMediTech, University of Tampere, Biokatu 6, FI-33520 Tampere, Finland
[c] Fimlab Laboratories, Biokatu 4, FI-33520 Tampere, Finland

ARTICLE INFO

Article history:
Received 8 October 2015
Received in revised form 8 February 2016
Accepted 10 February 2016
Available online 11 February 2016

Keywords:
Biosensor
Biotin surface
Avidin mutant
Reversible immobilization
Sensor chip regeneration

ABSTRACT

Biotinylated bait molecules can be immobilized on biotinylated sensor chips by formation of biotin–avidin–biotin bridges which are very stable when using wild-type (strept)avidin. Stable immobilization of biotinylated baits is important for monitoring reversible binding and dissociation of prey molecules. For measurements with another bait molecule, however, it is desirable to replace all immobilized proteins by fresh (strept)avidin and new biotinylated bait. In this study, five avidin mutants have been characterized with respect to their ability to form switchable biotin–avidin–biotin bridges on biotinylated chip surfaces, as needed for complete chip regeneration. All five mutants formed stable biotin–avidin–biotin bridges at pH 7, were more or less stable at pH 2–3, and required the combination of pH 2 with SDS for quantitative removal from the chip surface. Mutant #3 ("switchavidin") showed the best combination of properties, i.e., low nonspecific adsorption of protein and nucleic acids, high binding capacity, and good stability at pH 2–3, as typically used for quantitative removal of prey molecules in repeated measurement cycles.

1. Introduction

Biosensors monitor binding of soluble prey molecules to immobilized bait molecules. Subsequently, all bound prey molecules must be removed before the next sample can be measured [1]. Usually the bait molecules are immobilized by covalent bonds or by avidin–biotin interaction [2–5]. Since neither is reversible in a reasonable time window, a new measurement series can only be started after exchanging the sensor chip and immobilizing another bait molecule. A desirable alternative is replacement of the old bait molecules for new ones. Exchange of the bait on the chip confers significant advantages: (i) it saves the cost and time of chip exchange. (ii) No human intervention is required, allowing for switching of baits in programmed overnight runs. (iii) It eliminates chip-to-chip variation, which is a problem with some product lines. (iv) The most urgent need for in-situ exchange of bait molecules is encountered if the harsh conditions (e.g., 100 mM HCl or NaOH) typically used for removal of bound prey molecules [1] cause denaturation of the bait.

In order to be useful in practical application, any method of bait exchange must obey strict criteria: (a) the bait must remain stably bound for hours or days, until all planned measurements have been completed with one kind of bait molecule. (b) It must be possible to quantitatively remove all bound bait molecules within minutes. (c) The binding capacity for new bait molecules must be fully retained for a large number of regeneration cycles. (d) The reagents used for chip regeneration must be compatible with the flow cells of common biosensors. (e) The reagents and the chip surface must be stable under ambient conditions (i.e., not sensitive to oxidation or hydrolysis). (f) The sensor surface used for switchable bait immobilization must not bind any prey or side components of the sample. (g) Preferably, the method should be easy to implement in many types of biosensors.

Two published methods fulfill these criteria to a high degree. In both methods, avidin or (strept)avidin is reversibly immobilized, providing for immobilization of biotinylated bait molecules before a measurement series, and for rapid removal of (strept)avidin plus bait at the end. In the first method, (strept)avidin is

* Corresponding author.
E-mail address: hermann.gruber@jku.at (H.J. Gruber).

http://dx.doi.org/10.1016/j.snb.2016.02.039

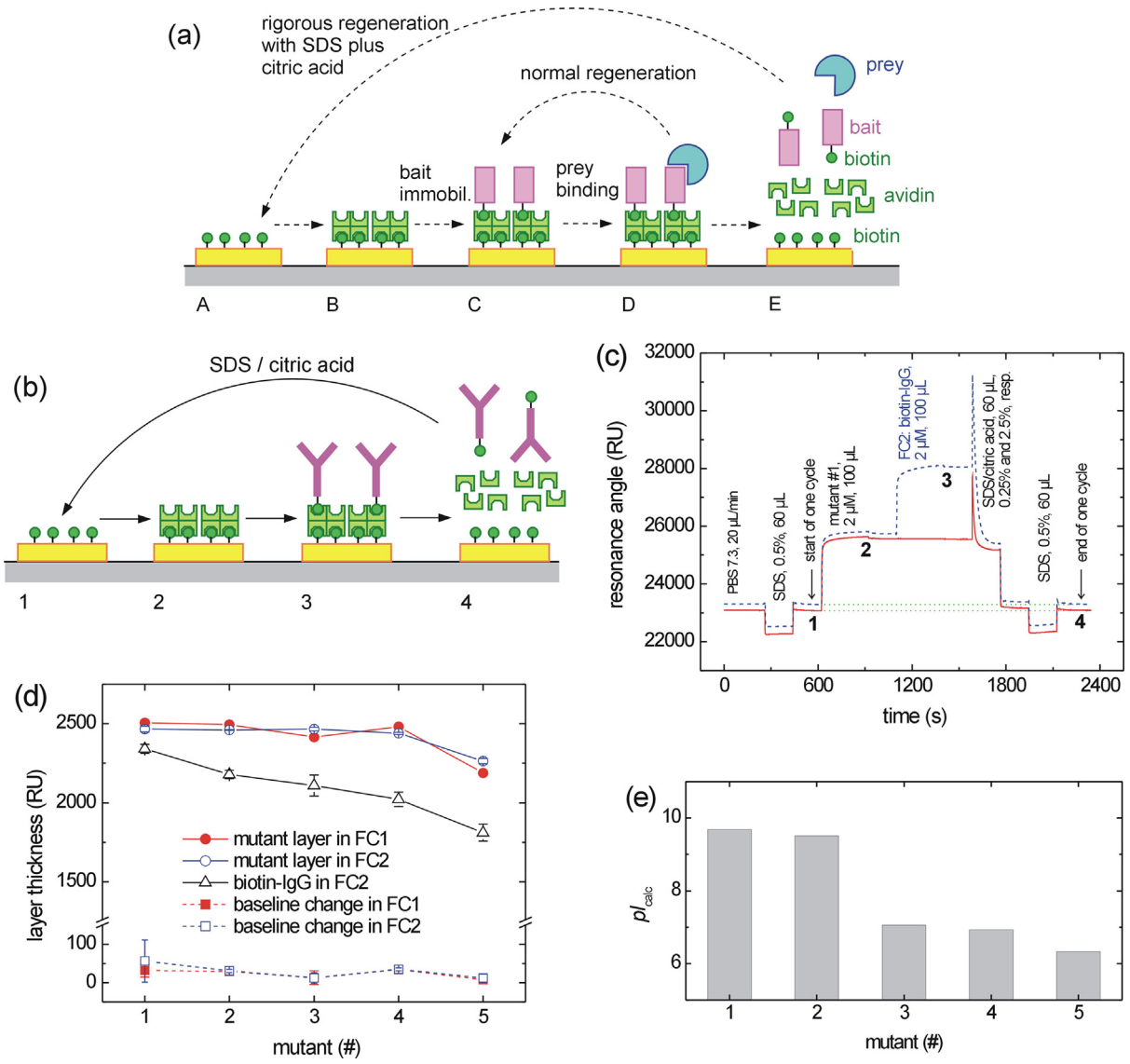

Fig. 1. Reversible functionalization of biotinylated sensor chips with biotinylated probe molecules. (a) Illustration of chip recycling with switchable biotin–avidin–biotin bridges. (b) Testing of different avidin mutants for reversible immobilization of biotinylated antibodies. (c) SPR traces showing binding of mutant #1 in both flow cells and of biotin–IgG in FC2 (blue dashed line), as well as removal by SDS/citric acid. The numbers 1–4 in (c) correspond to the stages 1–4 in (b). (d) Comparison with respect to the mutant layers in both cells, biotin–IgG bound in FC2, and baseline drift from stage 1 to 4. (e) Calculated *pI* of the avidin mutants (Table S1). (For interpretation of the references to color in this figure legend, the reader is referred to the web version of this article.)

reversibly immobilized on carboxymethyldextran via DNA double strand formation (BIAcore application note "Biotin CAPture Kit", GE data file 28-9577-47 AA, https://www.gelifesciences.com/gehcls_images/GELS/Related%20Content/Files/1314787424814/litdoc28957747AA1_20110831132219.pdf). This method fulfills criteria (a)–(e) but it is not applicable to DNA-binding proteins and only available for one brand of biosensors. In the second method, the avidin mutant M96H is used as a switchable link between biotinalyted sensor surfaces and biotinylated bait molecules [6,7]. Mutation M96H is located at the subunit interface (Supplementary Fig. S1) and it confers sensitivity to low pH [8]. In the biotin-bound state, however, this mutant retains full function down to pH 2.7, unless avidin M96H is intentionally dissociated into four nonfunctional subunits by combination of citric acid with sodium dodecyl sulfate (SDS) as outlined in Fig. 1a [6].

An obvious drawback of avidin M96H is its positive charge at neutral pH ($pI \sim 9.5$, see Fig. 1e). Most proteins and all nucleic acids are negatively charged at neutral pH, resulting in nonspecific adsorption to immobilized avidin M96H, especially in case of DNA [6,7]. Nonspecific protein adsorption was largely suppressed by blocking with biotin–BSA [6], whereas suppression of DNA adsorption required additional mutations, which lowered the *pI* towards 7 (mutant #3 in Fig. 1e and Table S1) [7].

In the present study, five avidin mutants (Table S1 and Fig. S1) were characterized along criteria (a)–(g) and the limits of the method were identified. Mutant #3 ("switchavidin" [7]) was found to be the optimal choice, combining high stability of the biotin–avidin–biotin bridge with low nonspecific adsorption of protein and DNA.

2. Materials and methods

2.1. Materials

The avidin mutants were constructed for bacterial expression in *Escherichia coli* by introducing mutations to cDNA encoding chicken avidin containing ompA signal peptide in pET101/D [9,10] by QuikChange mutagenesis according to manufacturer's

instructions (Stratagene, La Jolla, CA, USA) or by using standard PCR techniques, where multiple mutations were introduced by overlapping mutated DNA fragments amplified using DNA oligonucleotides containing the desired mutations, followed by subcloning to pET101/D with the help of TOPO cloning (for details see Ref. [7]). All DNA constructs were confirmed by DNA sequencing. The proteins were produced and purified as described [7]. The components of the mixed self-assembled monolayer (SAM) were synthesized and mixed as described in Ref. [6]. Biotin-cap-NHS, biotinylated protein G (biotin–protein G), immunoglobulin G (IgG) from goat, human IgG2κ, and lysozyme were obtained from Sigma–Aldrich. Bovine serum albumin (BSA, fatty acid-free) was purchased from Roche Applied Science. Biotin–IgG (with 6–7 biotins/IgG) was prepared as published [11] and biotin–BSA was prepared using the same mass concentrations of protein and biotin-cap-NHS. All single-stranded DNA molecules were custom-synthesized by VBC Genomics (Vienna) with 99 ± 0.5% coupling efficiency and the uncapped final product was purified by HPLC (positive selection for the 5′-terminal dimethoxytrityl group by reversed phase chromatography). The biotin-probe had the structure 5′-biotin-GCACCTGACTCCTGTGGAGAAGTCTGCCGT-3′ [5], the "unlabeled probe" had the same sequence but lacked biotin. The digoxigenin-labeled analyte was complementary to the probe (digoxigenin-5′-ACGGCAGACTTCTCCACAGGAGTCAGGTGC-3′) and the "unlabeled analyte" had the same sequence but lacked digoxigenin [5]. Biotin-N_{19}T contained 1:1:1:1 mixtures of A:C:G:T in positions 1–19 and thymine in position 20.

Phosphate-buffered saline (PBS 7.3) contained 140 mM NaCl, 2.7 mM KCl, 10 mM Na_2HPO_4, and 1.8 mM KH_2PO_4, yielding pH 7.3. It was degassed by sterile filtration (0.2 μm) with strong aspirator suction every day.

Biotin–BSA, Biotin–IgG, BSA, IgG, and lysozyme were purified by gel filtration in PBS 7.3 on Superdex 200 (1 × 30 cm, GE Healthcare) at 0.5 ml/min to remove aggregates. The protein concentrations were adjusted to 1 mg/ml and small aliquots were frozen in liquid nitrogen and stored at −25 °C. Biotin–protein G, IgG2κ and the oligonucleotides were dissolved in PBS (20 μM, 7 μM, and 10 μM, respectively) and stored at −25 °C. The aliquots were thawed by short immersion in water (~20 °C), diluted to the desired concentration by addition of PBS 7.3, stored at 4 °C, and used within four days.

2.2. Surface plasmon resonance experiments

Cleaning of bare glass chips, evaporation of chromium (3 nm) and gold (41 nm), as well as cleaning of the gold surface and coating with a mixed biotin SAM (Fig. S2) was performed as described [6]. The chips were mounted on the chip supports with double-sided adhesive tape (non-permanent) and inserted in a BIAcore X device for measurement of binding by surface plasmon resonance (SPR). Degassed buffer (PBS 7.3) was run over the chip surface at 10–20 μl/min, as stated in the figure legends. The resonance angle was recorded at 1 s intervals in both flow cells and expressed in resonance units (1 RU = 0.0001°).

3. Results and discussion

Fig. 1a shows the two kinds of chip regeneration used in this study. "Normal regeneration" means quantitative removal of prey molecules only, as conventionally performed on all kinds of biosensors [1]. "Rigorous regeneration" means quantitative dissociation of the biotin–avidin–biotin bridges on the chip surface, thereby recovering the bare biotinylated chip on which fresh avidin and a new kind biotinylated bait is immobilized for a new series of experiments. In this study, we examined the reproducibility of chip regeneration (Section 3.1), nonspecific binding of protein (Section 3.2) and nucleic acids (Section 3.6), multivalent bait–prey interactions (Section 3.3), as well as perfect differentiation between sample cell and reference cell (Section 3.5). Of particular interest was the suitability of methods for quantitative removal of prey ("normal regeneration") without losing biotinylated bait molecules from the chip surface (Section 3.4).

3.1. Binding of biotinylated protein to biotinylated surfaces by using different avidin mutants

In preceding studies [6,7], three different avidin mutants were shown to provide for reversible formation of biotin–avidin–biotin bridges, as outlined in Fig. 1a. Reversibility is made possible by mutation M96H which is located at the subunit interface (Fig. S1), causing subunit dissociation when treated with SDS/citric acid [6]. Mutant #2 contains the additional mutation R114L which lowers the *pI* value, reduces nonspecific binding, and enhances the affinity for biotinylated molecules [7], due to its location next to the biotin-binding site (Fig. S1). The three additional mutations in mutant #3 are located on the outer surface of avidin (Fig. S1, Table S1) and shifted the *pI* value towards 7 (Fig. 1e), resulting in very low nonspecific adsorption of proteins and nucleic acids [7].

In the present study, the newly prepared avidin mutant #4 was analogous to mutant #3, except that mutation R114L was replaced by mutation R26N which had little effect on the *pI* value (Fig. 1e). The intention was to demonstrate the beneficial effect of mutation R114L for the stability of the biotin-bound state, and this was confirmed by the data (see below). Finally, mutant #5 contained all mutations at the same time, causing further lowering of the *pI* value (Fig. 1e, Table S1).

Mutants #1–5 were systematically tested for their performance in reversible biosensor functionalization. The first test concerned binding of the avidin mutants to the biotinylated chip and of biotin–IgG on top of avidin (stages 2 and 3 in Fig. 1b), as well as removal of the bound proteins with a mixture of SDS and citric acid (stage 4 in Fig. 1b). As exemplified in Fig. 1c, the avidin mutant was injected in both flow cells and biotin–IgG in FC2 only. The experiments were performed in triplicates with all five avidin mutants and the signal amplitudes were highly reproducible (Fig. 1d).

The extent of mutant binding (stage 2 minus stage 1) was similar for mutants #1–4 (~2000 RU, circles in Fig. 1d), only mutant #5 was less effective. Binding of biotin–IgG (stage 3 minus stage 2) showed a significant decrease with increased mutant number (triangles in Fig. 1d). All mutants allowed for good reversibility of binding (stage 4 minus stage 1, squares in Fig. 1d). Mutant #3 performed best in this respect, with a drift of 13 ± 18 RU in FC1 and 13 ± 14 RU in FC2.

It is important to note that all tested chips could be regenerated for an unlimited number of cycles, except that the binding capacity of the chips started to decrease after three weeks of continued use.

3.2. Nonspecific adsorption of protein on monolayers of different avidin mutants

Sensitive and selective biosensing implies that no binding/adsorption of any component of the sample occurs on the chip surface, except for specific capture of prey to bait. Fig. 2a exemplifies the standard test [6] which consists of consecutive injections of lysozyme, BSA, and goat IgG.

The results for BSA and IgG are summarized in Fig. 2b. Mutant #3 showed the lowest adsorption of BSA (circles) and IgG (trian-

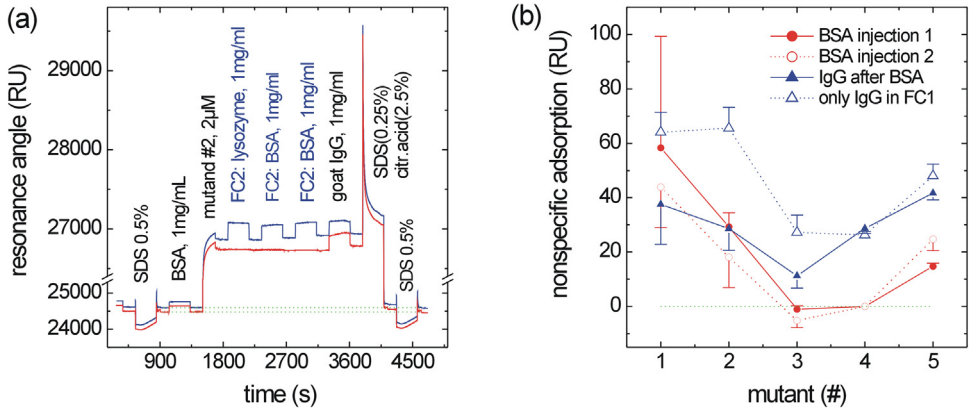

Fig. 2. Non-specific adsorption of proteins on monolayers of the avidin mutants #1–5. (a) Test for protein adsorption to mutant #2. (b) The experiment in (a) was performed with mutants #1–5. The amounts of protein which remained bound at the end of the injections of BSA and goat IgG are shown. "BSA injection 2" and "IgG after BSA" for mutants #1–3 were reported before [7].

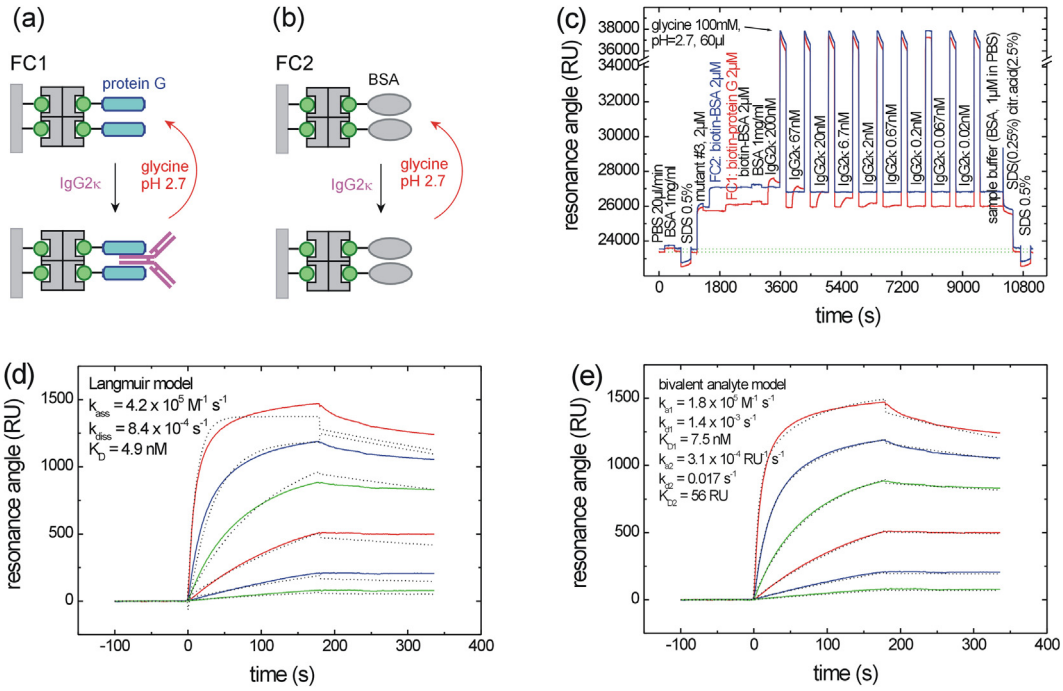

Fig. 3. Kinetics of human IgG2κ binding to biotin–protein G on top of mutant #3. (a) Schematic of binding to immobilized protein G in FC1 (red trace in (c)). (b) Schematic of the control injection in FC2 (blue trace in (c)). (c) Repeated association and dissociation of IgG2κ, using 100 mM glycine (pH 2.7) for removal of IgG2κ. The different IgG2κ samples were prepared by serial dilution of 7 µM IgG2κ (in PBS 7.3) with sample buffer (1 µM BSA in PBS 7.3). Double referencing [6,14] was used to obtain the experimental binding curves (solid traces in (d) and (e)). (d) The dotted lines show the best global fit of the Langmuir model to the experimental binding curves (solid lines). (e) Analogous fit as in (d), using the "bivalent analyte model". (For interpretation of the references to color in this figure legend, the reader is referred to the web version of this article.)

gles). The data set "IgG after BSA" is more relevant than "only IgG in FC1" because BSA is often used to passivate the chip surface before/during injection of samples (see Fig. 3). On mutant #3, binding of IgG amounted to 11 ± 5 RU after BSA and 27 ± 6 RU without BSA treatment, corresponding to 0.4% or 1% of an IgG monolayer, respectively [12]. Only a small amount of lysozyme was adsorbed on any avidin mutant (Fig. S3), due to the high *pI* value of lysozyme (11.2 [13]).

3.3. *Biological interaction analysis on avidin mutant-functionalized chip surfaces*

In a preceding study [6] we showed that biotinylated protein G and human IgG2κ provide for a critical functional test of chip performance, for two reasons: (i) the interaction is multivalent in the sense that one soluble IgG molecule is captured by two biotinylated protein G molecules on the chip surface (Fig. 3a). (ii) In this case, the repeated removal of IgG after each IgG injection (Fig. 3c) is typically performed with 100 mM glycine buffer (pH 2.7, GE Healthcare Data File 18-1012-91 AC, entitled "Affinity Chromatography: Protein G Sepharose 4 Fast Flow", available at the internet from https://www.gelifesciences.com/gehcls_images/GELS/Related%20Content/Files/1314774443672/litdoc18101291AC_20110831095008.pdf) which seems dangerously close to "rigorous regeneration" (Fig. 1a) with SDS/citric acid.

In Ref. [6] it was shown that the biotin–avidin–biotin bridges formed by mutant #1 were only affected by SDS/citric acid (pH 2.0) but not by glycine (pH 2.7). We now show that the same is also true for mutants #2 (Fig. S4c) and #3 (Fig. 3c). The avidin mutant under inspection was immobilized in both flow cells, FC2

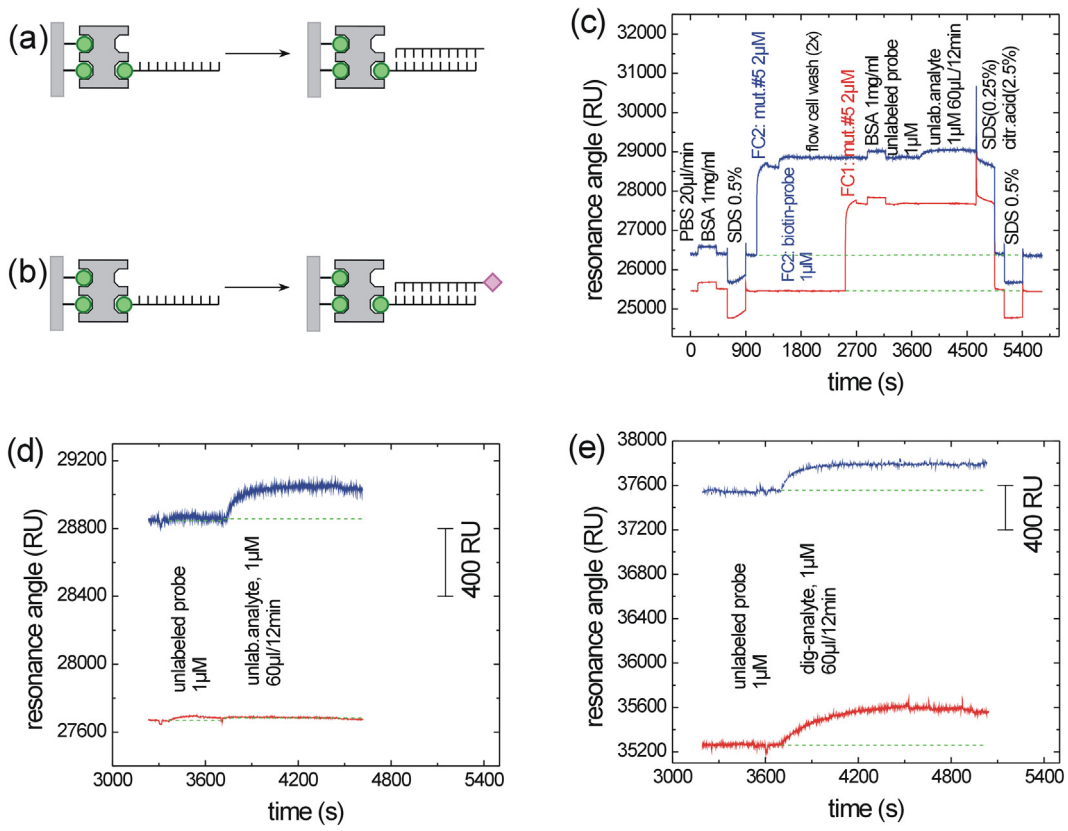

Fig. 4. Test for specific hybridization and non-specific adsorption of single-stranded DNA on mutant #5. (a) Schematic for hybridization of unlabeled analyte DNA, as used in (c). (b) Analogous schematic with digoxigenin-labeled analyte DNA. (c) Hybridization of unlabeled analyte DNA with complementary biotin-DNA which had been immobilized on mutant #5 in FC2 only (blue trace). (d) Segment from (c). (e) Analogous experiment as in (d), using digoxigenin-labeled analyte (compare (a) and (b)). (For interpretation of the references to color in this figure legend, the reader is referred to the web version of this article.)

was blocked with biotin–BSA (Fig. 3b) and FC1 was functionalized with biotin–protein G (Fig. 3a). After further passivation of both flow cells with biotin–BSA and BSA, different concentrations of IgG2κ were injected and repeatedly removed with glycine (pH 2.7), as shown in Fig. 3c. FC2 was subtracted from FC1 and the resulting trace for sample buffer injection (Fig. 3c) was subtracted from all other injection traces ("double referencing method" [14]), resulting in the experimental binding curves (solid traces in panels (d) and (e), Figs. 3 and S4). The kinetic data could well be fitted by the "bivalent analyte model" (Figs. 3 e and S4e, dotted lines), which assumes binding of each IgG molecule by two adjacent protein G molecules on the chip surface (Fig. 3a), in contrast to the simple Langmuir model (Figs. 3 d and S4d, dotted lines) which assumes 1:1 binding.

The usefulness of all three avidin mutants (#1–3) for biological interaction analysis is proven by the good agreement of the calculated kinetic constants (Table 1), yielding averages with small standard deviations (last column). In spite of the less perfect fit, the Langmuir model has the advantage that it yields an effective K_d value with the usual dimension "nM" (not "RU", as in the bivalent analyte model, see Table 1), allowing for comparison with literature data. K_d = 710 nM was reported from affinity adsorption of mixed human IgG [15]. The Fc fragment of human IgG1 gave K_d values of 47 nM in BIAcore experiments on a CM5 chip [16] and 310 nM in a homogeneous fluorescence assay [17]. The discrepancy with K_d = 2 nM in Table 1 is in part explained by the fact that bivalent interaction was only possible on our dense avidin monolayers which allow for close proximity of immobilized biotin–protein G (Fig. 3a). Obviously our chip is able to mimic the natural function of protein G, which is also present at high lateral density on the surface of *Streptococcus* sp. [18].

Table 1
Fit parameters of the Langmuir model (dotted curves in Fig. 3d) and of the bivalent analyte model (dotted curves in Fig. 3e) by which binding of human IgG2κ towards immobilized biotin–protein G (Fig. 3a) was analyzed on top of mutant #3. The corresponding data for mutant #2 are from Fig. S4, those for mutant #1 from Ref. [6].

Mutant	#1	#2	#3	#1–3
Langmuir model				
10^{-5} k_a M s	4.1	4.1	4.2	4.1 ± 0.1
10^4 k_d s	11	7.4	8.4	9.0 ± 1.9
K_D/nM	2.7	1.8	2.0	2.2 ± 0.5
R_{max}/RU	1370	1360	1290	1340 ± 44
Bival. analyte model				
10^{-5} k_{a1} M s	1.8	1.6	1.8	1.7 ± 0.1
10^4 k_{d1} s	17	14	14	15 ± 0.3
K_{D1}/nM	9.4	8.8	7.5	8.6 ± 0.9
10^4 k_{a2} RU s	1.7	2.7	3.1	2.5 ± 0.7
k_{d2} s	0.013	0.013	0.017	0.014 ± 0.003
K_{D2}/RU	77	47	56	60 ± 15
R_{max}/RU	1800	1930	1740	1820 ± 100

3.4. Sensitivity of avidin mutant-functionalized chips to acid or SDS

As mentioned above, the selective removal of IgG from protein G by 100 mM glycine (pH 2.7) in Fig. 3c seems rather close to the SDS/citric acid mixture (pH 2.0, Fig. S5) used for removal of all proteins at the end of Fig. 3c. A close look at the first IgG2κ injection indeed shows that the subsequent injection of glycine (pH 2.7) leads to a lower baseline (−188 RU) than before injection of 200 nM IgG2κ. Probably a small fraction of mutant #3 is more sensitive to pH 2.7 than the rest, being bound to only one biotin residue on

the biotin–SAM [19]. However, such baseline drift was not seen in the subsequent cycles with lower concentrations of IgG2κ. Thus, such a baseline shift during the bait–prey interaction study can easily be avoided when applying a dummy injection of glycine (pH 2.7) before the first injection of IgG2κ. The same observations were made with mutants #1 [6] and #2 (Fig. S4c).

Unfortunately, pH 2.7 is insufficient for removal of antigens from immobilized antibodies (or vice versa). Reported regeneration conditions range from pH 2.5 to pH 1.75 [1]. We, therefore, examined the resistance of the chip-bound avidin mutants #1–5 to low pH, using 2.5% citric acid without salt (pH 2.0) or with 150 mM NaCl (pH 1.9, Fig. S5). The results are shown in Figs. S6–S9. At pH 2, only mutant #1 showed stable binding to the biotinylated chip (red squares in Fig. S7b). Fortunately, the sensitivity to pH 2 was only seen if the avidin mutants were the only protein on the chip surface (state 2 in Fig. 1b). If biotinylated antibody was bound on top of avidin (state 3 in Fig. 1b) then all five avidin mutants were resistant to pH 2 (blue circles in Fig. S7b).

In spite of its lower pH (1.9, Fig. S5), the combination of citric acid with 150 mM NaCl caused much less removal of the avidin mutants from the biotinylated chip (Figs. S6–S9). A similar beneficial effect of elevated ionic strength is also expected for the 100 mM glycine buffers typically used for antibody–antigen separation.

Detergents are also used for removal of prey from bait [1]. Therefore, we tested the resistance of mutants #1–5 to 0.5% SDS at neutral pH (Figs. S10 and S11). Mutant #1 was very stable, while mutant #3 showed losses of ~5% (irrespective of whether biotin–IgG was bound on top of the avidin layer or not). Inclusion of NaCl afforded increased resistance to SDS.

The reported experiments with citric acid, NaCl, and SDS resulted in the following rules for "normal regeneration" (Fig. 1a) of chips functionalized with the tested avidin mutants:

i. The regeneration buffer (pH 1.9 or SDS) should have physiological ionic strength (e.g., 150 mM NaCl) because then much less avidin mutant (and biotinylated bait) is dissociated from the chip.
ii. Mutant #3 is most attractive because of low nonspecific adsorption, but this mutant will resist pH 1.9 only if it is crosslinked by a multiply biotinylated protein (sketch (d) in Fig. S7). Pronounced stabilization of avidin by such crosslinking has been demonstrated before [6]. This stabilization is high in case of IgG carrying 6–7 biotin residues on average (blue circles in Fig. S7b).
iii. The extent of crosslinking, and of stabilization at pH 1.9, will be much weaker in case of small proteins with few biotin residues and no stabilization is expected for baits with only one biotin residue. The latter situation is equivalent to a simple avidin monolayer (sketch (c) in Fig. S7). Here, only mutant #1 is sufficiently resistant to pH 1.9 (red squares in Fig. S7b). Fortunately, it is possible to eliminate nonspecific adsorption of protein on mutant #1 [6]. In case of DNA, however, it is necessary to use mutant #3 and other methods than pH 1.9 for "normal regeneration" (see Section 3.6).
iv. A small loss of avidin plus biotinylated bait will frequently be expected during the first regeneration round, even with milder regeneration at pH 2.7 (Fig. 3). Fortunately, no such loss is seen in subsequent injections. Therefore, a dummy injection with regeneration buffer should be performed before repeated binding and dissociation of prey molecules. Initial removal of the weekly bound avidin molecules has no adverse effects on subsequent measurement cycles of bait–prey interaction.

In conclusion, the choice of regeneration conditions and the choice of mutant #1 versus #3 must be made with care, in order to exploit the full potential of these mutants for regenerative biosensing.

3.5. How to prevent bait molecule immobilization in the reference cell

Label-free biosensing requires injection of the sample in the active cell with immobilized bait molecule and in a reference cell lacking the bait molecules (see Fig. 3a,b). Fig. 3c (and Fig. S12c) show that the bait (biotin–protein G) was only present in the sample cell if the reference cell was functionalized with biotin–BSA prior to injection of biotin–protein G to the active cell. In contrast, pronounced contamination of the reference cell with biotin–protein G was observed if protein G was injected before biotin–BSA (Fig. S12b). The reason lies in the design of microfluidic flow cells which allows for diffusion between the cells even if the flow is blocked in one cell (see Fig. S12a).

Fig. 4c shows another successful strategy by which bait immobilization is restricted to the active cell. Mutant #5 was first injected into the active cell only (FC2, blue trace in Fig. 4c), followed by injection of biotinylated bait (biotin-probe). In this situation, mutant #5 is still absent in the reference cell (FC1, red trace) and no biotin-DNA can be immobilized in FC1, even if a trace of it diffuses into FC1. Subsequently, mutant #5 was injected into the reference cell (FC1, red trace), generating an inert surface where no DNA was bound in the next steps.

The protocol in Fig. 4c always ensures restriction of bait to the active flow cell. The simpler protocol in Fig. 3c is only applicable to large baits (such as proteins) which cannot bind on avidin after injection of biotin–BSA.

3.6. Specific and nonspecific binding of DNA on avidin-mutant-functionalized chip surfaces

In a preceding study [7], mutants #1 and #2 exhibited high nonspecific adsorption of DNA, whereas only specific binding (hybridization, Fig. 4a) was seen on mutant #3. The same experiment was now performed on mutants #4 (Fig. S15) and #5 (Fig. 4c). The sample cell was functionalized with avidin and biotinylated probe DNA, followed by avidin binding in the reference cell. Subsequently, absence of nonspecific protein adsorption was seen with BSA and absence of nonspecific DNA adsorption when injecting unlabeled probe DNA which had same nucleotide sequence as the biotinylated DNA on the chip surface (Fig. 4c). Subsequent injection of unlabeled analyte DNA gave pronounced hybridization in the sample cell (blue traces in Fig. 4c and d) and no nonspecific response in the reference cell (red traces in Fig. 4c and d). However, when the experiment was repeated using digoxigenin-labeled DNA (Fig. 4b) in place of unlabeled DNA (Fig. 4a), pronounced binding was observed in the reference cell (red trace in Fig. 4e). No such effect was seen with mutant #4 (Fig. S15) and mutants #1–3 (see below) even when using digoxigenin-labeled DNA.

Fig. 5 compares mutants #1–4 with respect to specific binding (hybridization) and nonspecific adsorption. The top row (a)–(c) concerns experiments with mutant #1. Panel (a) shows pronounced binding of analyte DNA, both in the active cell which contained the complementary biotinylated probe DNA (blue trace), and in the reference cell with the bare monolayer of mutant #1 (red trace). We suspected that the contribution of nonspecific DNA adsorption in the active cell (blue trace) was much lower than the purely nonspecific signal in the reference cell (red trace), because the positively charged mutant #1 was covered with negatively charged biotin-DNA in the active cell but not in the reference cell. This hypothesis was verified in panel (b) where the reference cell contained a degenerated oligonucleotide (biotin-N_{19}T),

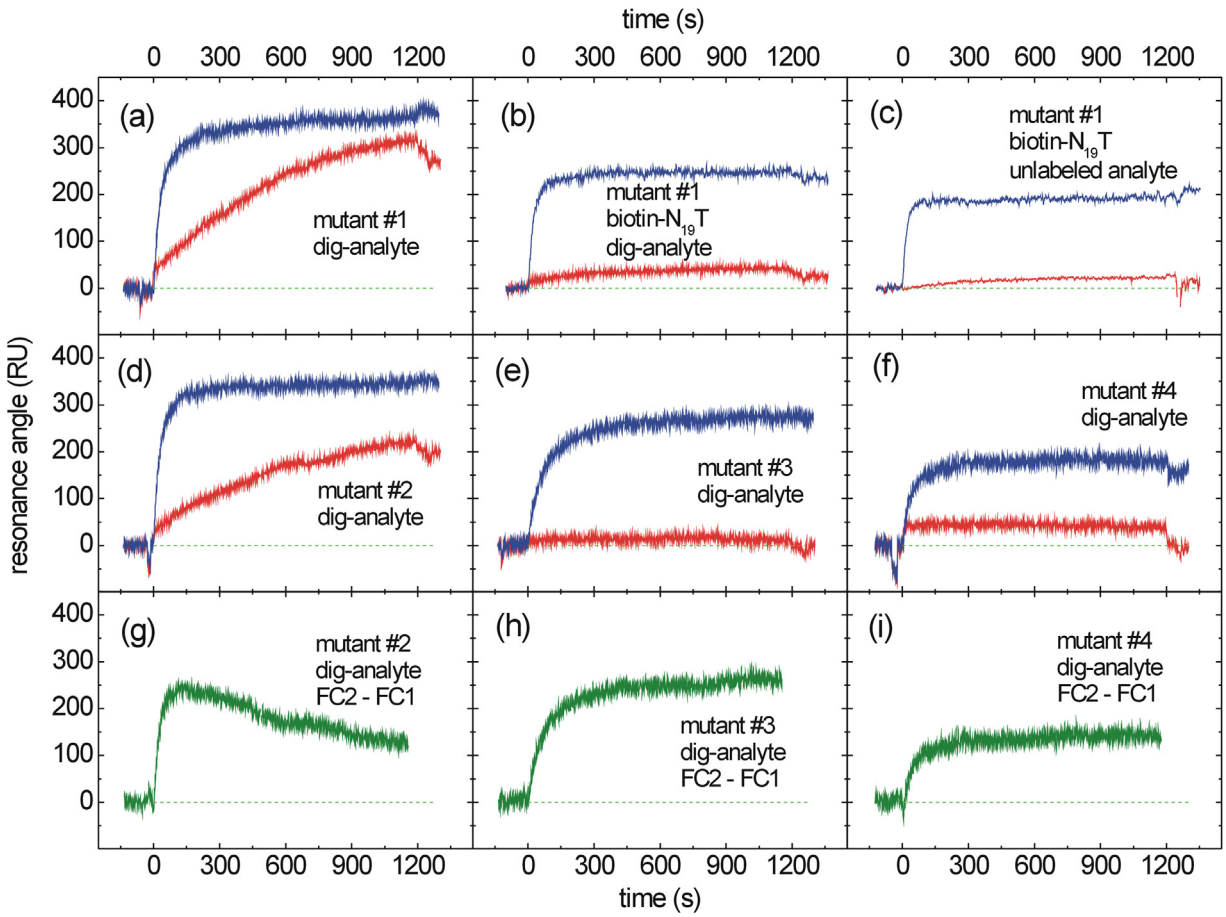

Fig. 5. DNA hybridization experiments performed on monolayers of mutant #1 (panels a–c), and of mutants #2, #3, and #4 (panels d–f), using the protocol of Fig. 4c. Red traces show adsorption of analyte DNA to the avidin mutants in FC1, blue traces the sum of specific and nonspecific binding in FC2 to avidin carrying biotin-labeled probe DNA. The green traces in (g), (h), and (i) were calculated by subtraction of the red traces from the blue traces in (d), (e), and (f), respectively. The analyte DNA always carried a digoxigenin label, except in (c). In (b) and (c) both flow cells were treated with biotin-N_{19}T before injection of analyte DNA. (For interpretation of the references to color in this figure legend, the reader is referred to the web version of this article.)

while the active cell contained biotinylated probe DNA plus subsequently injected biotin-N_{19}T. This resulted in low nonspecific binding not only in the reference cell (red trace) but also in the active cell (blue trace). Panel (c) confirms the beneficial effect of biotin-N_{19}T and a very minor contribution of the digoxigenin label to nonspecific adsorption of digoxigenin-labeled DNA to mutant #1.

The center row (d)–(f) shows the performance of mutants #2–4 under the same conditions as used for mutant #1 in panel (a) (i.e., with digoxigenin-labeled DNA, in absence of biotin-N_{19}T). Nonspecific binding of DNA on mutant #2 (red trace in (d)) was only slightly lower than on mutant #1. Nonspecific DNA adsorption was absent on mutants #3 and #4 (red traces in (e) and (f)). The small transient displacement of the red trace in panel (f) is due to a bulk effect (different refractory index of sample and running buffer). The findings are well explained by the high *pI* values of mutants #1 and #2 (Fig. 1e), which implies a positive net charge, and by the neutral *pI* of mutants #3 and 4, which eliminates electrostatic attraction of DNA.

The bottom row (g)–(i) shows the extent of specific binding (hybridization), as calculated by subtraction of nonspecific binding in the reference cell (red traces in (d)–(f)) from total DNA binding in the active cell (blue traces in (d)–(f)). The biphasic curve for mutant #2 (panel (g)) is caused by much higher nonspecific adsorption in the reference cell than in the active cell (as explained above for mutant #1). In contrast, panels (h) and (i) reflect the true hybridization signals on mutants #3 and #4, due to absence of nonspecific adsorption on both mutants (red traces in (e) and (f)). Mutant #3 exhibits a higher binding capacity than mutant #4, therefore it appears best suited for measurement of DNA-containing samples.

In this study we provide no method for the "normal regeneration" (Fig. 1a) of DNA-functionalized chips, i.e., for complete dissociation of analyte DNA without loss of biotinylated DNA. Mutant #3 is not sufficiently stable to use 100 mM HCl (as used in the "Biotin CAPture Kit") and the more acid-resistant mutant #1 strongly adsorbs DNA. The most promising reagent seems concentrated urea; it ensures complete dissociation of DNA duplexes [20], while avidin is known to resist 9 M urea without losing its biotin-binding capacity [21]. However, establishing the exact conditions will require a substantial amount of experiments in a future study.

4. Conclusions

All five tested avidin mutants are suitable for reversible immobilization of biotinylated baits on biotinylated sensor chips. The stably formed biotin–avidin–biotin bridges can be quantitatively dissolved when desired.

Mutant #1 showed the highest stability at pH 2 and the highest binding capacity for biotinylated bait molecules. Nonspecific binding of proteins was moderate, especially when biotin–BSA was used to passivate the reference cell and the unoccupied biotin-binding sites in the active cell. The major weakness of mutant #1 was high

nonspecific binding of nucleic acids. Passivation with degenerate biotin-N_{19}T caused a strong reduction of DNA adsorption but did not eliminate it completely. In conclusion, mutant #1 may be ideal for biological interaction analysis between purified proteins, but it appears unsuitable for biosensing where nucleic acids are likely to be present. Mutant #2 resembles mutant #1 in all respects, except that all positive and negative aspects are somewhat moderated.

Mutant #3 showed slightly lower binding capacity and stability at pH 2, nevertheless it can well be used for interaction studies between antibodies and antigens where pH 2.3 is typically used for repeated removal of the analyte. The reason is that statistically biotinylated antibodies or antigens cause crosslinking of mutant #3, which confers high stability down to pH 2. This fact is important because mutant #3 appeared ideal in all other aspects: it showed the lowest nonspecific binding of protein and DNA and the highest performance in chip recycling with SDS/citric acid.

Mutants #4 and #5 exhibited also low nonspecific binding of protein and DNA. However, they were not stable at pH 2 and their binding capacity for biotinylated bait molecules was considerably lower than that of mutant #3. In conclusion, mutant #3 showed the best overall performance in chip recycling and application of recycled chips in biosensing.

Acknowledgements

This work was supported by the government of Upper Austria (project DK Nanocell) and by grants from the Academy of Finland (project numbers 136288 and 140978 to V.P.H.). We acknowledge the infrastructure support by Biocenter Finland. We thank Sandra Posch and Felix Faschinger for helpful comments on the manuscript.

Appendix A. Supplementary data

Supplementary data associated with this article can be found, in the online version, at http://dx.doi.org/10.1016/j.snb.2016.02.039

References

[1] J.A. Goode, J.V.H. Rushworth, P.A. Millner, Langmuir 31 (2015) 6267–6276.
[2] M.A. Cooper, Sensor surfaces and receptor deposition, in: M.A. Cooper (Ed.), Label-free Biosensors, 1st ed., Cambridge University Press, Cambridge, New York, Melbourne, Madrid, Cape Town, Singapore, Sao Paolo, Delhi, 2009, pp. 110–142.
[3] B. Johnsson, S. Lofas, G. Lindquist, A. Edstrom, R.M. Müller-Hillgren, A. Hansson, J. Mol. Recognit. 8 (1995) 125–131.
[4] J.-I. Sawada, F. Suzuki, DNA-protein interactions, in: K. Nagata, H. Handa (Eds.), Real-time Analysis of Biomolecular Interactions, Springer Publishing Co., Tokyo, 2000, pp. 127–132.
[5] X.D. Su, Y.J. Wu, R. Robelek, W. Knoll, Langmuir 21 (2005) 348–353.
[6] P. Pollheimer, B. Taskinen, A. Scherfler, S. Gusenkov, M. Creus, P. Wiesauer, D. Zauner, W. Schöfberger, C. Schwarzinger, A. Ebner, R. Tampé, H. Stutz, V.P. Hytönen, H.J. Gruber, Bioconjug. Chem. 24 (2013) 1656–1668.
[7] B. Taskinen, D. Zauner, S.I. Lehtonen, M. Koskinen, C. Thomson, N. Kähkönen, S. Kukkurainen, J.A.E. Määttä, T.O. Ihalainen, M.S. Kulomaa, H.J. Gruber, V.P. Hytönen, Bioconjug. Chem. 25 (2014) 2233–2243.
[8] H.R. Nordlund, V.P. Hytönen, O.H. Laitinen, S.T. Uotila, E.A. Niskanen, J. Savolainen, E. Porkka, M.S. Kulomaa, FEBS Lett. 555 (2003) 449–454.
[9] V.P. Hytönen, O.H. Laitinen, T.T. Airenne, H. Kidron, N.J. Meltola, E.J. Porkka, J. Hörhä, T. Paldanius, J.A.E. Määttä, H.R. Nordlund, M.S. Johnson, T.A. Salminen, K.J. Airenne, S. Ylä-Herttuala, M.S. Kulomaa, Biochem. J. 384 (2004) 385–390.
[10] J.A. Määttä, Y. Eisenberg-Domovich, H.R. Nordlund, R. Hayouka, M.S. Kulomaa, O. Livnah, V.P. Hytönen, Biotechnol. Bioeng. 108 (2011) 481–490.
[11] A.S.M. Kamruzzahan, A. Ebner, L. Wildling, F. Kienberger, C.K. Riener, C.D. Hahn, P.D. Pollheimer, P. Winklehner, M. Hölzl, B. Lackner, D.M. Schörkl, P. Hinterdorfer, H.J. Gruber, Bioconjug. Chem. 17 (2006) 1473–1481.
[12] J. Lahiri, L. Isaacs, J. Tien, G.M. Whitesides, Anal. Chem. 71 (1999) 777–790.
[13] A. Kondo, K. Higashitani, J. Coll. Int. Sci. 150 (1992) 344–351.
[14] R.L. Rich, D.G. Myszka, Curr. Opin. Biotechnol. 11 (2000) 54–61.
[15] T.V. Gupalova, O.V. Lojkina, V.G. Palagnuk, A.A. Totolian, T.B. Tennikov, J. Chromatogr. A 949 (2002) 185–193.
[16] S. Radaev, P.D. Sun, J. Biol. Chem. 276 (2001) 16478–16483.
[17] K.N. Walker, S.P. Bottomley, A.G. Popplewell, B.J. Sutton, M.G. Gore, Biochem. J. 310 (1995) 177–184.
[18] S.R. Fahnestock, P. Alexander, J. Nagle, D. Filpula, J. Bacteriol. 167 (1986) 870–880.
[19] L.S. Jung, K.E. Nelson, P.S. Stayton, C.T. Campbell, Langmuir 16 (2000) 9421–9432.
[20] Southern, E.M. 2002. Denaturing gel electrophoresis of RNA and DNA using urea-polyacrylamide gel. In: eLS. John Wiley & Sons Ltd., Chichester. http://www.els.net/WileyCDA/ElsArticle/refId-a0003778.html. [doi: 10.1038/npg.els.0003778].
[21] N.M. Green, Biochem. J. 89 (1963) 609–620.

Biographies

Dominik Zauner received his M.Sc. degree from the Institute of Organic Chemistry at Johannes Kepler University Linz, Linz, Austria, in 2015. He did his master thesis as guest of Prof. Hermann J. Gruber (see below) where he synthesized new components for self-assembled monolayers and characterized their use for renewable biosensor surfaces.

Barbara Taskinen received her B.Sc. degree (2006) and her M.Sc. degree (2008) in Biochemistry at the University of Berne, Berne, Switzerland. She did her Ph.D. thesis in the group of Prof. Vesa P. Hytönen at BioMediTech at the University of Tampere, Tampere, Finland and received her Ph.D. degree in Medical Technology and Biotechnology (2014). Since 2014 she is a postdoctoral fellow at the University of Washington, Department of Genome Sciences, Seattle, USA where she studies the evolution of tyrosine kinases.

Daniel Eichinger received his B.Sc. degree in Medical Engineering at the University of Applied Sciences of Upper Austria, Linz, Austria, in 2013. He did his bachelor thesis as guest of Prof. Hermann J. Gruber (see below).

Clemens Flattinger received his B.Sc. degree in Medical Engineering at the University of Applied Sciences of Upper Austria, Linz, Austria, in 2013. He did his bachelor thesis as guest of Prof. Hermann J. Gruber (see below).

Bianca Ruttmann did her bachelor studies in "Biological Chemistry", a joint study program of the University of South Bohemia, Budejovice, Czech Republic, and of Johannes Kepler University Linz, Linz, Austria. She received her Bachelor degree from the Institute of Inorganic Chemistry at Johannes Kepler University Linz, Linz, Austria (2012). Her master studies were in "Molecular Biosciences", a joint study program of the Paris Lodron University, Salzburg, Austria, and of Johannes Kepler University Linz, Linz, Austria where she received her M.Sc. degree in 2014. Her master thesis in the group of Prof. Hermann J. Gruber (see below) was concerned with new fluorescent biotin derivatives and with renewable sensor surfaces. Presently she is product engineer at GE Healthcare, Linz, Austria.

Claudia Knoglinger received her B.Sc. degree in Microbiology and Genetics from the University of Vienna in 2013 and her M.Sc. degree in Molecular Biology (with emphasis on Biochemistry) in 2015 from the same university. From 2014–2015 she did her master thesis as guest of Prof. Hermann J. Gruber, Institute of Biophysics, Johannes Kepler University Linz (Austria), characterizing different strategies for sensor surface regeneration. Presently she is product engineer at GE Healthcare, Linz, Austria.

Lukas Traxler received his B.Sc. degree (2011) and his M.Sc. degree (2013) in Medical Engineering from the University of Applied Sciences of Upper Austria, Linz, Austria. He did his master thesis as guest of Dr. Andreas Ebner (Institute of Biophysics, Johannes Kepler University Linz, Linz, Austria) in the field of biosensing (QCM and SPR). In 2014 he received a M.Sc. degree in Law and Economics from Johannes Kepler University Linz, Linz, Austria. Presently he is a Ph.D. student of Prof. Hermann J. Gruber in the Ph.D. Program "Nanocell", a joint program of Johannes Kepler University Linz, Linz, Austria, of the Institute of Science and Technology, Klosterneuburg, Austria, and of Vienna University of Technology, Vienna, Austria.

Andreas Ebner received his Ph.D. in Technical Sciences at the Institute of Biophysics at the Johannes Kepler University (JKU) Linz, Austria in 2007. He worked as software developer for Ebner Engineering (1991–1999), as research associate at the Institute of Biophysics JKU (2000) and at the Upper Austrian Research (2000–2001). Furthermore he was scientific consultant for Amersham Biosciences (2002–2003) and was employed as scientific assistant by Molecular Imaging, USA. At the institute of biophysics he is group leader (since 2007) and assistant professor (since 2011). He published >70 peer reviewed scientific articles, and >10 scientific book chapters. His key competences are biosensing atomic force microscopy techniques like single molecule force spectroscopy and recognition imaging.

Hermann J. Gruber received his Ph.D. in chemistry from the Institute of Organic Chemistry at Karl–Franzens–University in Graz, Austria in 1983. He was postdoctoral fellow in the group of Prof. P. S. Low in the Biochemistry Division of the Chemistry Department at Purdue University, West Lafayette (1983–1985) and in the group of Prof. H. Schindler at the Institute of Biophysics of Johannes Kepler University Linz, Linz, Austria (1985–1995), whereupon he became assistant professor (1995–2001) and associate professor (since 2001) at the same institute. He has published >130 scientific articles. In particular, he established a toolbox of linkers and procedures for flexible tethering of single biomolecules to the measuring tip of force micro-

scopes and published many studies on new fluorescent biotin derivatives and their application in Bioanalytics. Presently he develops renewable sensor surfaces that facilitate biosensing and biological interaction analysis.

Vesa P. Hytönen is head of the Protein Dynamics research group and acts as a lecturer in BioMediTech at the University of Tampere, Tampere, Finland. After graduating as a Ph.D. from the University of Jyväskylä, Jyväskylä, Finland at 2005, he conducted postdoctoral training at ETH Zurich, Zürich, Switzerland (2005–2007). He then continued as a postdoctoral researcher at the University of Tampere and established an independent research group at 2010. His research interests are mechanobiology, protein engineering and vaccine research, and he has published >90 scientific articles.